



Sensitivity of the Ni-W nanocomposite doped amorphous nano-SiO₂ particles to the electrolysis pH

W. Sassi^{1,2,*}, L. Dhouibi², P. Berçot², M. Rezrazi²

¹Equipe COPROMET, Unité de Recherche Mécanique-Energétique, ENIT, Université de Tunis El-Manar, Tunisie.

²Institut UTINAM, CNRS UMR 6213, Université de Franche-Comté, 16 route de Gray, 25030 Besançon Cedex, France

Received 25 Jan 2015, Revised 12 May 2015, Accepted 12 May 2015

*Corresponding Author. E-mail: ing.wafa.sassi@gmail.com; Tel: (+21622587558)

Abstract

In spite of the nanoscale coatings progress, the effect of bath pH on nano silica zeta potential, surface morphology and electrochemical behavior of pulse electroplated Ni-W/SiO₂ nanocomposite from citrate-ammonia media were investigated. Zêta potential curve and SEM analysis shows that the nanocomposite coatings obtained were smoother, more compact and with finer grain size. Corrosion resistance and electrochemical behavior into 3% NaCl media were discussed. The enhancement of the Ni-W/SiO₂ nanocomposite has been referred to the mechanism of the formation of the nanoparticles adions double layer.

Keywords: Copper, SiO₂ nanoparticles, Corrosion.

1. Introduction

With the development of nanotechnology, a number of literatures reported SiC, ZrO₂, Al₂O₃ and TiO₂ nanoparticles, which were added to the plating bath and could be co-deposited with metal or alloy to form nanocomposite coatings (1-4). Among the insoluble nanoparticles used for reinforcement, SiO₂ is frequently studied and applied for its properties such as high hardness (5), good oxidation resistance (6, 7) and good chemical stability (8). Nevertheless, due to the nanometric particle size, the SiO₂ species agglomerated very easily in the plating bath which promotes conglomeration phenomena on deposited alloys and elaboration of nanocomposite coatings failed. Therefore, dispersion of these particles in the plating bath is an important parameter which is affected by nanoparticles concentration in the plating bath and stirring rate (1-4). In this work, Ni-W/SiO₂ nanocomposite coatings were electroplated from a nickel-tungsten plating bath containing SiO₂ nanoparticles. The electroless pH effect on nano-SiO₂ particles incorporation mechanism and corrosion behavior of Ni-W alloy was investigated.

2. Materials and methods

2.1. Zêta potential measurements

Zêta potential measurements were obtained using a standard laboratory instrument using an optical technique (Zetasizer 3000HS Advance, Malvern Instrument GmbH, UK). This equipment measures distribution of electrophoretic mobility and Zêta potential of nano-SiO₂ particles in liquid suspensions using Laser Doppler Velocimetry (LDV).

2.2. Operating conditions

After preliminary tests, the Ni-W/SiO₂ nanocomposite electrodeposition was realized by pulsed current. The pulsed parameters were:

$$j = -15 \text{ mA cm}^{-2}; t_{\text{on}} = 48.5 \text{ ms}; t_{\text{off}} = 1.5 \text{ ms} \quad (\text{Eq.1})$$

where j is the applied current density, t_{on} is the time of cathodic pulse (on-time) and t_{off} is the time between pulses (off-time). Experiments were conducted at room temperature (25±2°C). Ni-W/SiO₂ nanocomposites were electroplated from the same aqueous solutions described elsewhere (9).

2.3. Apparatus and methods

Scanning Electron Microscopy (SEM) was carried out using a JEOL type 5600 (9-12). The distribution of species in the deposit was determined by depth profiling with Glow discharge optical emission spectroscopy (GDOES) technique (9-12). The polarization curves were obtained by means of a potentiostat–galvanostat Radiometer Copenhagen PGZ 402 model, piloted by software Voltlab4 (9-12)(1-4).

3. Results and discussion

3.1. pH of the electroplating bath

In Figure 1, there is plotted Zêtapotential evolution of SiO₂ suspensions into Ni-W electroplating bath at different pH values.

We can easily note that the stability of amorphous nanoparticles SiO₂ is effectively dependent of pH within the pH range observed for our study (i.e., 1 < pH < 6.8). However, for the studied nanoSiO₂, predicted Zêta potentials are considerably higher at diluted electroplating bath than apparent Zêta potentials (13). This large underestimation of the predicted Zêta potential at the Ni-W electroplating bath is due to the presence of different charged species into the solution and the very high surface electrical conductivity of SiO₂ nanoparticles (13).

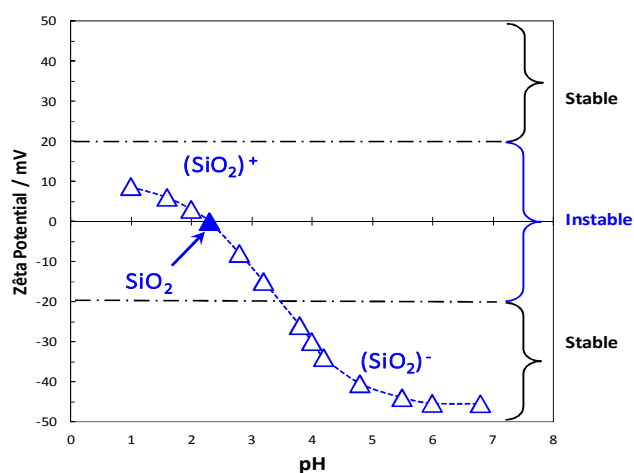


Figure 1: Zeta-potential as a function of pH for the amorphous nano-SiO₂ dispersed into the electroplating bath Ni-W alloy.

The PZC (point zero charge) of amorphous SiO₂ in this conditions is around pH = 2.3, the Zêtapotential is positive below the PZC (SiO₂H₄²⁺ are the dominant species) and negative above the PZC (SiO₂²⁻ are the dominant species). The pH of our Ni-W electroplating bath optimized elsewhere (10) is around 4. At this pH value, Figure 1 shows negatively charged nanoparticles of SiO₂. This type of oxide is hydrophilic, so it always interacts with the electrolyte, and therefore chemical and physical adsorption of electrolyte ions onto the particle occurs. This adsorption and the initial particle surface composition determine the particle surface charge, which induces a double layer of electrolyte ions around the particle. In electrolytes, double layers play a major role in the interactions between particles and also between particles and the electrode (11-12). It can be seen from Figure 1 that, in pH 4, the value of zeta potential was lower than 20 mV. In order to confirm our hypothesis, we choose another pH value (pH 3) closed to the pH 4 but make the Zêtapotential reaching the instable area of SiO₂ nanoparticles. On the other hand, the variation of pH from 3 to 4 did not affect the proprieties of the Ni-W coating alloy (10-12). The Zêtapotential related to this pH (pH 3) is about 14 mV. One should also note that the nanoparticles are negatively charged at this pH range.

3.2. Coatings morphology

The metallic structure of our films is shown in Figure 2. The SEM observations of the pulsed Ni-W alloys obtained at pH 3 and 4 (Figure 2-A and -B, respectively) show that the Ni-W layers were found gray, shining and cover the totality of the surfaces. Both of dry coatings present a quiet different granulated morphology with

well-defined grains of around $1\mu\text{m}$ in size (Figure 2-A and -B). This similarity confirms that the variation of pH by one unit did not make change on the surface morphology of the Ni-W alloy.

Whereas, SEM micrographs recorded after addition of nano SiO_2 into electroplating bath present a totally different microstructure (Figure 2-C and -D). Indeed, nanocomposite electroplated at pH 3 keeps the same morphology as free silica nanoparticles bath; showing well defined small grains on the background (Figure 2-C). But one should also note the presence of a glass palate like-structure. At this fragment on Figure 2-C, EDS spectrum recorded a higher silicon presence (unreported result). Therefore, this structure has been referred to the adsorption of amorphous silica agglomerate according to a similar morphology observed and verified elsewhere (10-12). On the other hand, the SEM micrograph of Ni-W/ SiO_2 nanocomposite coated at pH 4 (Figure 2-D) shows a uniform, continuous and compact morphology. Moreover, Figure 2-D is also characterized by much nodular shiny structure with relatively big grains of about $1.6\mu\text{m}$. This observation indicates that the codeposited SiO_2 nanoparticles are much uniformly incorporated and distributed into the Ni-W matrix of the nanocomposite coating obtained at pH 4.

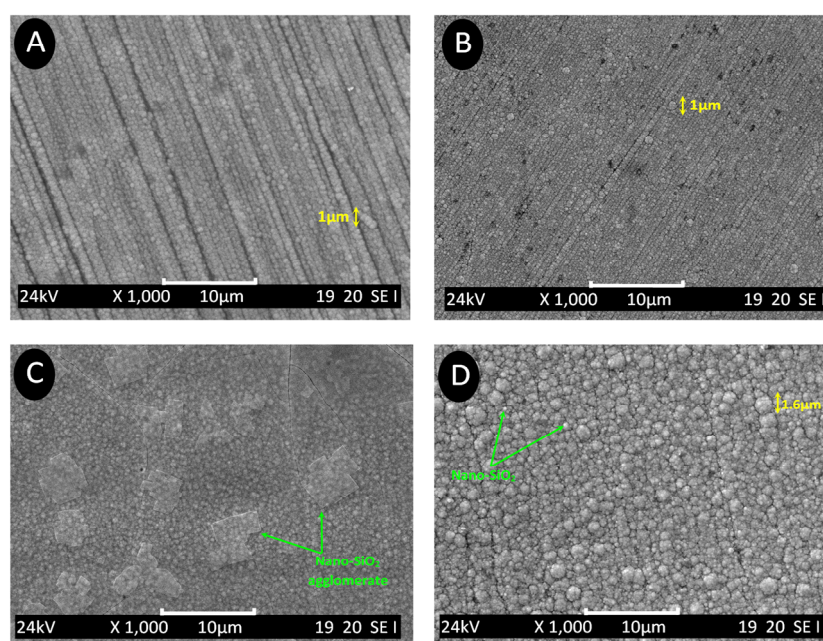


Figure 2. SEM micrographs of Ni-W coatings electroplated at (A): pH 3, (B): pH 4 and Ni-W/ SiO_2 nanocomposite coatings electroplated at (C): pH 3, (D): pH 4.

3.3. Interface electrochemical behavior

Figure 3 gives the open circuit potential curves against time into 3% NaCl. The open circuit potentials of Ni-W films electroplated at pH 3 and pH 4 show similar behaviors. One should note that this similarity confirms that the variation of pH by one unit did not make change on coating proprieties (9-12). Whereas, the Ni-W/ SiO_2 nanocomposite alloys obtained at pH 3 and at pH 4 didn't behave in similar manner. The curve of the nanocomposite electroplated at pH 3 slowly decreased from potential value of around -50 until reaching -72 mV/SCE and this could imply in a slow dissolution. On the other hand, the nanocomposite electroplating at pH 4 seems to be more stable into 3% NaCl when its curve present a linear aspect which prove that no dissolution is detected during immersion time into chloride media. This observation reveals the good protection of the incorporation of SiO_2 nanoparticles by improving free potentials of Ni-W nanocomposite electroplated at pH 4 into 3% NaCl solution. To address the protective properties of the coatings, we have also recorded potentiodynamic polarization curves in 3% NaCl solution.

Polarization curves of the specimens tested in 3 % NaCl electrolyte with pH 3 and 4 are shown in Figure 4. For free nanoparticles Ni-W films curves, the potentiodynamic plots are shifted towards higher currents when

compared to those of coatings obtained from electrolyte containing amorphous nano-SiO₂. The cathodic branch of all samples reveals a Tafel slope corresponding to the simultaneous reduction of oxygen and protons H⁺ (10-12). Nevertheless, a small cathodic peak has been observed on Ni-W/nano SiO₂ (electroplated at pH 4) polarization at about -200mV/SCE (Figure 4). Indeed, it has been related to a parallel reduction of species onto active surface (probably amorphous SiO₂ and related complexes). On the other hand, the corrosion currents of Ni-W alloys are higher than those obtained with Ni-W/SiO₂ nanocomposite coatings by a factor of 100.

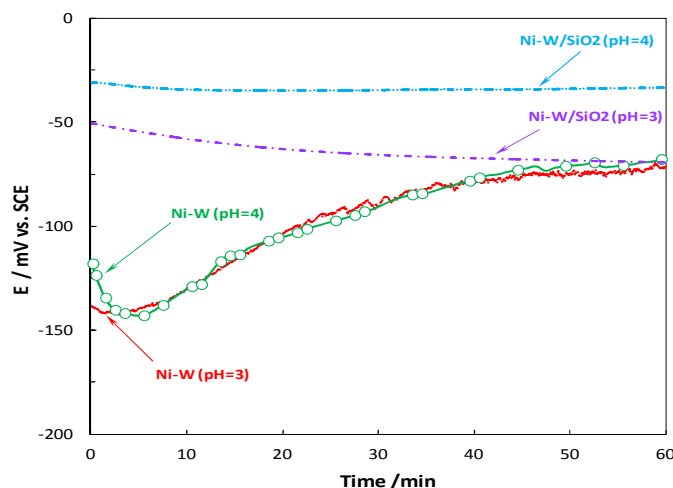


Figure 3. Open circuit potential (dE/dt) into 3% NaCl of Ni-W coatings and Ni-W/SiO₂ nanocomposite coatings both electroplated at pH 3 and pH 4.

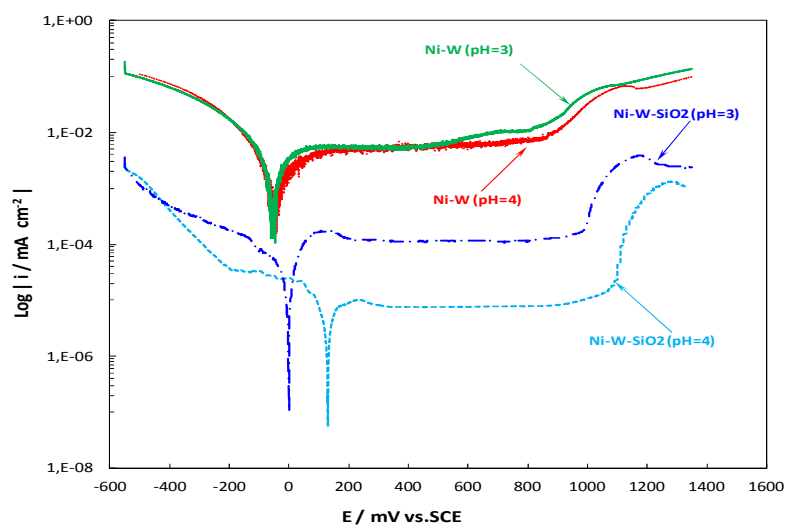


Figure 4. Polarization curves into 3% NaCl of Ni-W coatings and Ni-W/SiO₂ nanocomposite coatings both electroplated at pH 3 and pH 4.

Moreover, it is obvious that at different pH (3 and 4) the corrosion behavior of the tested nanocomposites alloys is different. In Figure 4, the nanocomposite plated at pH 4 shows higher E_{corr} than nanocomposite obtained at pH 3. This means that the electroless pH 4 gives protective nanocomposite coating with better general corrosion resistance than those at obtained pH 3. Therefore, we can deduce that the addition of amorphous SiO₂ nanoparticles into electroplating bath (with an adjusted pH 4) decreases the dissolution rate of the Ni-W composites coatings.

Conclusions

- 1) The zêta potential of studied nano-SiO₂ into Ni-W media shows a negative surface charge of the nanoparticles. The limit between stability and instability has been confirmed.
- 2) At pH 4, the electroplated Ni-W/SiO₂ nanocomposite alloy where homogenous with well defined grains and compact structure. While layer obtained from pH 3 media show a smooth background with finer grains and presence of "glass plates" referred to nano-SiO₂ agglomerates.
- 3) SEM and GDOES studies show that the nanocomposite electroplated at pH 4 is smoother, thicker, more compact, homogenous and harder when compared to the film obtained at pH 3.
- 5) The Ni-W/SiO₂ nanocomposite coatings in both cases (pH 3 or 4) improve electrochemical properties of copper substrate.

Acknowledgements - The authors would like to acknowledge the financial support provided by "Action Intégrée Franco-Tunisienne du Ministère des Affaires Etrangères et Européennes français et du Ministère de l'Enseignement Supérieur, de la Recherche Scientifique et de la Technologie tunisien".

References

1. Hou K. H., Chang Y. F., Chang S. M., Chang C. H., *Thin Film* 518 (2010) 7535.
2. Metikos-Hukovic M., Grubac Z., Radic N., Tonejc A., *J. Mol. Catal. A-Chem.* 249 (2006) 172.
3. Rupert J. T., Schuh C. A., *Acta Materialia* 58 (2010) 4137.
4. Wang H., Liu R., Cheng F., Cao Y., Ding G., Zhao X., *Microelectron. Eng.* 87 (2010) 1901.
5. Mai P., Fang W., Liu G., Chan Y., He S., Li J., *Materials Letters*, 65 (2011) 3496.
6. Eliaz N., Sridhar T. M., Gileadi E., *Electrochim. Acta* 500 (2012) 2893.
7. Kollia C., Spyrellis N., Amblard J., Froment M., Maurin G. M., *J. Appl. Electrochem.* 20 (1990) 1025.
8. Vedove W. D. Sanfeld A., *J. Colloid Interf. Sci.* 84 (1981) 328.
9. Sassi W., Dhoubi L., Berçot P., Rezrazi M., Triki E., *Electrochim. Acta* 117 (2014) 443.
10. Sassi W., Dhoubi L., Berçot P., Rezrazi M., Triki E., *Appl. Surf. Sci.* 263 (2012) 373.
11. Sassi W., Dhoubi L., Berçot P., Rezrazi M., *Appl. Surf. Sci.* 324 (2015) 369.
12. Sassi W., Dhoubi L., Berçot P., Rezrazi M., Triki E., *Surf. Coat. Technol.* 206 (2012) 4235.
13. Leroy P., Devau N., Revil A., Bizi M., *J. Colloid Interf. Sci.* 410 (2013) 81.

(2015) ; <http://www.jmaterenvironsci.com>